

Reduced-Order Modeling of a Lithium-Ion Lithium Iron Phosphate Battery

Michael T. Castro^a, Joey D. Ocon^{a,b,*}

^a Laboratory of Electrochemical Engineering (LEE), Department of Chemical Engineering, University of the Philippines Diliman, Quezon City 1101, Philippines

^b Energy Engineering Program, National Graduate School of Engineering, College of Engineering, University of the Philippines Diliman, Quezon City 1101, Philippines
 jdocon@up.edu.ph

Battery energy storage systems are essential for stabilizing the intermittent power generation of renewable energy (RE) technologies. Their integration into RE systems is typically studied using energy systems modeling software that utilize either idealized models or complex models that require experimental data. Reduced-order modeling offers minimal experimental costs through the use of a multiphysics model in lieu of experimental battery data. In this work, a previously reported multiphysics model of a lithium-ion lithium iron phosphate (Li-ion LFP) battery was simulated in COMSOL Multiphysics® and reduced into an equivalent circuit model (ECM). The reduced-order ECM was then implemented as a battery systems model in an energy systems modeling tool to perform RE-based hybridization studies. Techno-economic case studies were conducted on RE-based systems powering a household and an off-grid island to validate the reduced-order ECM with the idealized battery model with HOMER Pro. Optimal component sizes computed using the two software generally showed good agreement and deviations were attributed to electrical losses. The state of charge (SOC) vs. time graphs generated by the two software had an average root mean square error of 0.00173 SOC units across the different case studies. Discrepancies were observed during rapid charging or high SOC values, which were characteristic of the reduced-order ECM. This model reduction framework can be applied to other energy storage and conversion technologies, such as other Li-ion chemistries, fuel cells, and supercapacitors, to generate chemistry-specific models for energy systems research.

1. Introduction

The world is undergoing a renewable energy (RE) transition. The rapidly decreasing costs of RE technologies, such as solar photovoltaics (PV) (Schmidt et al., 2017), has prompted their integration into existing energy infrastructure. At the center of the RE transition are energy storage systems, which address the intermittency of RE through peak shaving and frequency stabilization functions. The lithium-ion (Li-ion) battery, particularly the lithium iron phosphate (LFP) chemistry, has excelled in this purpose due to its safety and low cost (Xu et al., 2015). The effects of the RE transition can be seen in off-grid areas where RE technologies have been deployed to reduce dependence on diesel generators (Bertheau and Blechinger, 2018).

The study of RE-based systems entails a techno-economic optimization wherein the sizes (i.e., energy and power ratings) of the components are determined such that the electricity generation costs are minimized under the constraint that electricity is supplied continuously (Bertheau and Blechinger, 2018). The calculations are performed using energy systems modeling software, which simulate the supply and demand of energy between the energy components and the electrical load. In most cases, an idealized battery model is assumed wherein the battery is modeled as a reservoir of energy while electrical losses are simulated using constant charge and discharge efficiencies (Anoune et al., 2018). The oversimplification in this model is necessary as several hundred charge and discharge cycles are usually considered during an energy system simulation. More advanced models include the internal resistance model (He et al., 2011), which accounts for electrical losses through a series resistance. These models typically require empirical parameters that must be determined through experimental methods, which can be costly and time-consuming.

These limitations are partially addressed by multiphysics modeling, wherein the battery is simulated based on fundamental laws in chemistry and physics. This modeling technique accurately predicts electrochemical properties at the continuum scale (Xu et al., 2015). Moreover, experimental data is necessary only for physical property estimation and model validation, many of which have already been published in literature.

Multiphysics modeling is too computationally expensive for energy systems simulations. This has motivated the development of reduced-order models, wherein a multiphysics model is simplified to enable its application in large-scale studies. Equivalent circuit models (ECM), such as the internal resistance model discussed earlier, qualify as reduced-order models if the parameters are obtained from multiphysics models instead of experimental data. This reduces the computational cost by at least an order of magnitude (Li et al., 2019). In this work, a reduced-order ECM for Li-ion LFP was developed for use in energy systems modeling. This model reduction framework can be extended to other energy storage systems for the development chemistry-specific models for energy systems research.

2. Methodology

The methodology is divided into four steps. First, a Li-ion LFP multiphysics model reported in literature was replicated in COMSOL Multiphysics®. Second, the multiphysics model was reduced into an ECM. Third, the reduced-order ECM was implemented in Island Systems LCOE_{min} Algorithm (ISLA), an in-house energy systems modeling tool (Castro et al., 2020). Finally, case studies were conducted to compare the reduced-order ECMs and the idealized battery model.

2.1 Multiphysics modeling

The multiphysics model used in this work was based on the 16.5 Ah prismatic Li-ion LFP battery reported by Xu et al. (2015). The battery was modeled by coupling a pseudo-2D (P2D) electrochemical model describing one layer of current collectors, electrodes, and the separator and a 3D thermal model describing the whole prismatic battery. The coupling was performed by setting the average heat generation of the P2D electrochemical model as the heat generation of the 3D thermal model and setting the average temperature of the 3D thermal model as the temperature of the P2D electrochemical model. The modeling parameters used in this study are presented in Table 1. The multiphysics model was then validated with experimental data reported by Xu et al. (2015) for discharge curves at 0.5C and 1C under convective cooling. Energy systems modeling studies restrict the C-rate of a Li-ion battery below 1C (Bertheau, 2020), so simulating higher C-rates is unnecessary.

Table 1: Multiphysics modeling parameters

Parameter	Anode CC	Anode	Separator	Cathode	Cathode CC
Solid volume fraction	1	0.56	0.46 [a]	0.435	1
Liquid volume fraction	0	0.3	0.54 [a]	0.28	0
Solid initial concentration [mol/m ³]		25,221 [*]		984.21 [*]	
Solid max. concentration [mol/m ³]		31,370 [a]		26,390	
Solid electrical conductivity [S/m]	6.33×10 ⁷ [a]	100		0.5 [a]	3.83×10 ⁷ [a]
Liquid transport number		0.363	0.363	0.363	
Liquid diffusion coefficient [m ² /s]		from [a]	from [a]	from [a]	
Entropy [V/K]		from [b]		from [a]	

[*] Adjusted to fit experimental data, [a] (Samba et al., 2014), [b] (Rheinfeld et al., 2019). Parameters without citations were taken from (Xu et al., 2015). "CC" refers to the current collectors.

2.2 Reduction to ECM

The 1st order RC model shown in Figure 1 was considered as the ECM in this work. It contains a voltage element, a series resistance, and a RC loop. This model was selected because the RC loop provides a transient response unlike the internal resistance model, which only contains a series resistor, but has less complexity than the 2nd order RC model, which contains two RC loops. The voltage predicted by a 1st order RC model is given by Eq(1) and Eq(2).

$$V(t) = V_0 - I(t)R_0 - V_1(t) \quad (1)$$

$$\frac{dV_1(t)}{dt} = -\frac{V_1(t)}{R_1C_1} + \frac{I(t)}{C_1} \quad (2)$$

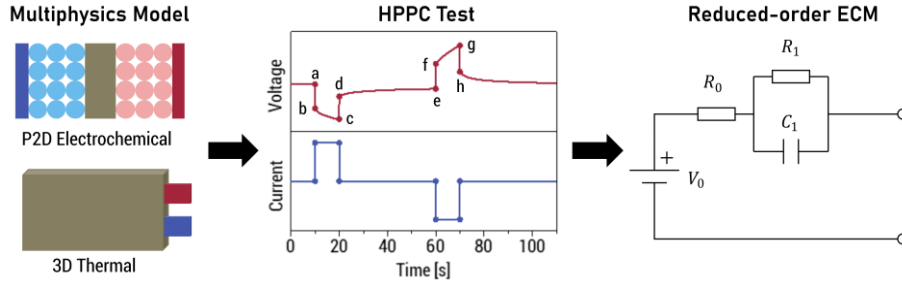


Figure 1: The HPPC test is applied to the multiphysics model to generate the reduced-order ECM.

The impedances were determined via the hybrid pulse power characterization (HPPC) test. First, the state of charge (SOC) of the battery was lowered to the desired amount by rebalancing the solid phase Li^+ concentrations. Next, the current pulse in Figure 1 was applied to the multiphysics model. The impedances were then determined from the corresponding voltage response using the methodology outlined by Huo et al. (2020). The impedance parameters were obtained at 30 °C and 50 % SOC. The temperature was selected as it is a target in many battery cooling systems (Alaoui, 2017), while the SOC was arbitrarily selected due to the weak dependence of the impedance parameters on the SOC (Huo et al., 2020). This work assumes a constant temperature of 30 °C, but the effects of temperature can be included in future work.

2.3 Implementation in ISLA

To implement the reduced-order ECM in ISLA, the power vs. current and current vs. SOC relations must be determined. A relation between the power and current was derived from Eq(3). Because this equation was solved several thousand times during the energy system optimization, the integral was simplified by assuming that the open circuit voltage is a linear piecewise function of the discharged capacity. Eq(3) was also used to convert the maximum current due to C-rate or SOC restrictions into a maximum power value, which was considered by ISLA when the power to be charged or discharged from the battery was calculated. The current obtained from Eq(3) was also used to update the SOC as given by Eq(4).

$$P(t) = I(t)[V_0(Q(t)) - I(t)R_0 - V_1(t)] \quad (3)$$

$$\text{SOC}(t + \Delta t) = \text{SOC}(t) - \frac{I(t)\Delta t}{Q_{nom}} \quad (4)$$

2.4 Case studies

The implementation of the reduced-order ECM was validated by conducting case studies on energy systems for the off-grid Lubid Island, Palawan, Philippines (11.0 °N, 120.7 °E) and a representative household served by the Manila Electric Railroad and Light Company (MERALCO). The scenarios considered in each case study are summarized in Table 2.

Table 2: Scenarios for each case study

Case Study	Scenario	Description	Simulation Sizes
Island	PV-HRES	Hybrid renewable energy system (HRES) with solar PV, Li-ion, and diesel.	40 kW solar PV, 50 kWh Li-ion, 36 kW diesel
	HRES	HRES with solar PV, wind, Li-ion, and diesel.	40 kW solar PV, 40 kW wind, 50 kWh Li-ion, 36 kW diesel
	PV-RE	100 % RE with solar PV and Li-ion.	200 kW solar PV, 500 kWh Li-ion
	RE	100 % RE with solar PV, wind, and Li-ion.	200 kW solar PV, 40 kW wind, 500 kWh Li-ion
Household	Grid-tied	Solar PV and Li-ion system connected to the grid.	
	RE	100 % RE system with solar PV and Li-ion.	

The validation was performed in two parts. First, a techno-economic optimization of the energy systems was performed using ISLA and HOMER Pro (Homer Energy, 2021), which contained the reduced-order ECMs and idealized battery model, respectively. The modeling and optimization in ISLA are discussed in a previous

publication (Castro et al., 2020). The optimum sizes and levelized cost of electricity (LCOE) calculated by both software were then compared. Second, the energy systems were simulated in ISLA and HOMER Pro under the condition that the component sizes were given by the “Simulation Sizes” column in Table 2. The SOC vs. time curves generated by both models were then compared based on the root mean square error (RSME). The techno-economic data used in the calculations are presented in Table 3. The load profile of the household was taken from MERALCO, while that of the island was estimated from the peak demand estimation methodology by Meschede et al. (2019) and the normalized load profiles by Bertheau and Blechinger (2018). The global horizontal irradiance and wind speed at 10 m in both areas were obtained from Phil-LiDAR 2 (Blanco et al., 2015). The hub height of the wind turbines was also at 10 m, so no wind speed corrections were necessary.

Table 3: Techno-economic assumptions

Component	Parameter	Value	Ref.	Component	Parameter	Value	Ref.
Solar PV	CapEx [USD/kW]	1,500	[a]	Diesel	CapEx [USD/kW]	500	[b]
	OpEx [USD/kW·y]	15	[a]		OpEx [USD/kW·h]	0.03	[*]
	Lifetime [y]	20	[a]		Lifetime [h]	15,000	[*]
Wind	CapEx [USD/kW]	2,500	[a]	Grid	Min. load ratio [%]	25	[*]
	OpEx [USD/kW·y]	62.5	[a]		Fuel cost [USD/L]	0.9	[c]
	Lifetime [y]	20	[a]		Rate [USD/kWh]	0.2	[d]
Li-ion	CapEx [USD/kWh]	700	[a]	Project	CapEx [USD]	0	[a]
	OpEx [USD/kWh·y]	5	[a]		OpEx [USD/y]	0	[a]
	Lifetime [y]	10	[a]		Discount rate [%]	8	[a]
	Roundtrip η [%]	90	[a]		Lifetime [y]	20	[a]

[*] Default input in HOMER Pro (Homer Energy, 2021), [a] (Bertheau, 2020), [b] (Bertheau and Cader, 2019), [c] (Ocon and Bertheau, 2019), [d] Typical electricity price from MERALCO.

3. Results and discussion

The results and discussion section is divided into three parts. First, the validation of the multiphysics model is presented. Second, the impedance parameters obtained from the HPPC test are shown. Lastly, the reduced-order ECMs and the idealized battery model are compared.

3.1 Multiphysics modeling

The calculated and experimental voltage curves are compared in Figure 2. The voltage curves predicted by the multiphysics model agreed well with experimental data. There was some deviation at 0.5C towards the end of discharge, but this was acceptable as the battery is operated above 20 % SOC in energy systems studies.

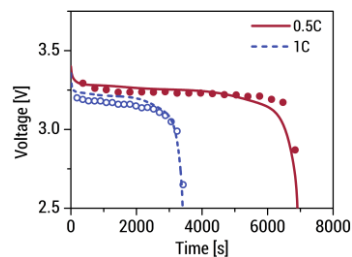


Figure 2: Comparison of calculated (line) and experimental (points) voltage of the 16.5 Ah Li-ion LFP battery under 0.5C (red, solid) and 1C (blue, dashed) discharge and convective cooling.

3.2 Reduction to ECM

The impedance parameters calculated from the HPPC were $R_0 = 449.23$ m Ω ; $R_1 = 84.37$ m Ω ; and $C_1 = 190.93$ F. The R_1 and C_1 values were within the baseline prescribed by Zhou et al. (2021). As for the high value of R_0 , it should be noted that these impedance parameters described one layer of current collectors, electrodes, and the separator. The resistance of the battery should be lower as these layers are connected in parallel.

3.3 Case studies

The techno-economic optimization results are presented in Table 4. The component sizes calculated by ISLA and HOMER Pro for the scenarios showed good agreement, although there were deviations that suggest energy

losses attributed to the ECM. For instance, the scenarios involving wind and the household load profile called for larger installations of the Li-ion battery. This is due to power spikes introduced by wind turbines or present in the household load profile that contributed to a sharp increase in demand, which increased the current and the incurred losses. More batteries are therefore required to compensate for these losses.

Table 4: Techno-economic optimization results

Scenario	PV [kW]	Wind [kW]	Li-ion [kWh]	Diesel [kW]	LCOE [USD/kWh]	Scenario	PV [kW]	Li-ion [kWh]	Diesel [kW]	LCOE [USD/kWh]
PV-HRES	38.1		20.3	35.5	0.403	PV-RE	184.0		362.9	0.611
	38.9		19.0	36.0	0.410		174.0		387.0	0.619
	-2.1 %		6.8 %	-1.4 %	-1.7 %		5.7 %		-6.2 %	-1.3 %
HRES	24.7	30.9	27.2	35.5	0.345	RE	164.6	17.3	312.1	0.577
	25.4	32.0	27.0	36.0	0.358		176.0	6.0	312.0	0.568
	-2.8 %	-3.4 %	0.7 %	-1.4 %	-3.6 %		-6.5 %	188.3 %	0.0 %	1.6 %
Scenario						Scenario				
Grid-tied	0.091		0.000		0.183	RE	0.54		1.71	0.615
	0.094		0.000		0.176		0.56		1.69	0.616
	-3.2 %		0.0 %		4.0 %		-3.4 %		1.1 %	-0.2 %

Top row – ISLA, middle row – HOMER Pro, bottom row – relative error of ISLA vs. HOMER Pro. Negative values indicate that ISLA predicted lower values than HOMER Pro.

The SOC vs. time curves calculated by ISLA and HOMER Pro for the off-grid case study, along with their differences (i.e., ISLA minus HOMER Pro), are presented in Figure 3. The PV-HRES, HRES, PV-RE, and RE scenarios had RSMES of 0.00145, 0.00179, 0.00215, and 0.00153 SOC units, respectively. In the PV-RE and RE scenarios, ISLA estimated higher SOC values than HOMER Pro. This is due to the higher battery voltage at higher SOC, which corresponds to a reduced current and slower changes in the SOC. The low current also minimizes the effect of the internal resistances. In contrast, ISLA predicts lower SOC values at higher currents as evidenced by the PV-HRES and HRES scenarios due to electrical losses.

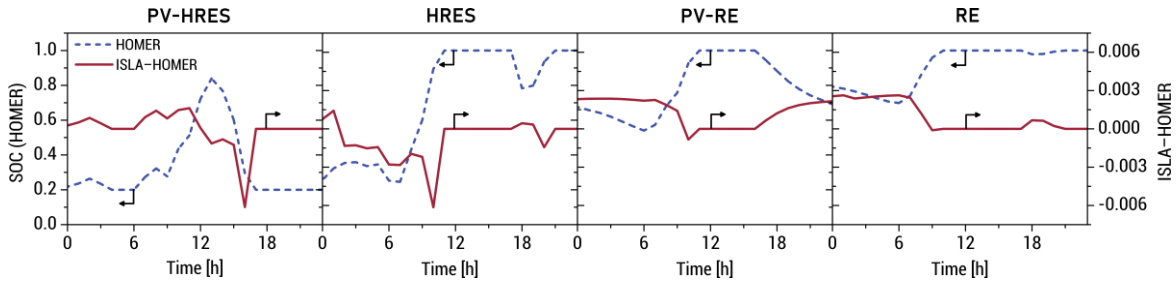


Figure 3: SOC vs. time curves generated by HOMER Pro (blue, dashed) during one representative day, and the SOC calculated by ISLA minus that of HOMER Pro (red, solid).

4. Conclusions

In this work, a multiphysics model of a Li-ion LFP battery was reduced into an ECM for use in energy systems modeling. The case studies and verification with HOMER Pro showed that the optimum sizes calculated by the reduced-order ECM were mostly within 5 % of those predicted by the idealized battery model, although there were deviations attributed to electrical losses. The SOC vs. time curves were generally in agreement but showed deviations characteristic of the reduced-order ECM. The results suggest that reduced-order ECMs must be used over the idealized battery model, especially in storage technologies with larger energy losses than Li-ion LFP. This study demonstrated a model reduction framework for developing a battery model for energy systems research via reduced-order modeling. The framework minimizes the cost of experimental activities by using a multiphysics model and published experimental data. This is valuable for developing chemistry-specific models for the energy systems modeling of expensive technologies such as hydrogen fuel cells.

Nomenclature

C_1 – RC loop capacitance, F
 I – current, A

P – power, kW
 Q – discharged capacity, Ah

Q_{nom} – nominal capacity, Ah	Δt – timestep, h
R_0 – series resistance, Ω	V_0 – open circuit voltage, V
R_1 – RC loop resistance, Ω	V_1 – RC loop voltage, V
t – time, s	

Acknowledgements

M.T.C. would like to acknowledge the Engineering Research and Development for Technology (ERDT) Graduate Scholarship. J.D.O. would like to acknowledge the ElectriPHI Program funded by the University of the Philippines Office of the Vice-President for Academic Affairs, and the Center for Advanced Batteries Program funded by the Department of Science and Technology (DOST) through the Niche Centers in the Regions for R&D (NICER) Program.

References

- Alaoui C., 2017, Thermal management for energy storage system for smart grid, *Journal of Energy Storage*, 13, 313–24.
- Anoune K., Bouya M., Astito A., Abdellah A.B., 2018, Sizing methods and optimization techniques for PV-wind based hybrid renewable energy system: A review, *Renewable and Sustainable Energy Reviews*, 93, 652–73.
- Bertheau P., 2020, Supplying not electrified islands with 100% renewable energy based micro grids: A geospatial and techno-economic analysis for the Philippines, *Energy*, 202, 117670.
- Bertheau P., Blechinger P., 2018, Resilient solar energy island supply to support SDG7 on the Philippines: Techno-economic optimized electrification strategy for small islands, *Utilities Policy*, 54, 55–77.
- Bertheau P., Cader C., 2019, Electricity sector planning for the Philippine islands: Considering centralized and decentralized supply options, *Applied Energy*, 251, 113393.
- Blanco A.C., Tamondong A.M., Perez A.M.C., Ang M.R.C.O., Paringit E.C., 2015, The Phil-LiDAR 2 program: National resource inventory of the Philippines using LiDAR and other remotely sensed data, *International Archives of the Photogrammetry, Remote Sensing and Spatial Information Sciences*, 40, 1123–1127.
- Castro M.T., Alcanzare M.T., Esparcia E.A., Ocon J.D., 2020, A comparative techno-economic analysis of different desalination technologies in off-grid islands, *Energies*, 13(9), 2261.
- He H., Xiong R., Fan J., 2011, Evaluation of lithium-ion battery equivalent circuit models for state of charge estimation by an experimental approach, *Energies*, 4, 582–598.
- HOMER Energy, 2021, HOMER Pro 3.14 User Manual, <www.homerenergy.com/products/pro/docs/latest/index.html> accessed 06.08.2021.
- Huo Y.T., Hu W., Li Z., Rao Z., 2020, Research on parameter identification and state of charge estimation of improved equivalent circuit model of Li-ion battery based on temperature effects for battery thermal management, *International Journal of Energy Research*, 44, 11583–11596.
- Li Y., Vilathgamuwa M., Farrell T., Choi S.S., Tran N.T., Teague J., 2019, A physics-based distributed-parameter equivalent circuit model for lithium-ion batteries, *Electrochim Acta*, 299, 451–69.
- Meschede H., Esparcia E.A., Holzapfel P., Bertheau P., Ang R.C., Blanco A.C., Ocon J.D., 2019, On the transferability of smart energy systems on off-grid islands using cluster analysis – A case study for the Philippine archipelago, *Applied Energy*, 251, 113290.
- Ocon J.D., Bertheau P., 2019, energy transition from diesel-based to solar photovoltaics-battery-diesel hybrid system-based island grids in the Philippines – Techno-economic potential and policy implication on missionary electrification, *Journal of Sustainable Development of Energy, Water and Environment Systems*, 7, 139–154.
- Rheinfeld A., Sturm J., Noel A., Wilhelm J., Kriston A., Pfrang A., Jossen A., 2019, Quasi-isothermal external short circuit tests applied to lithium-ion cells: Part II, modeling and simulation, *Journal of The Electrochemical Society*, 166, A151–A177.
- Samba A., Omar N., Gualous H., Capron O., Van Den Bossche P., Van Mierlo J., 2014, Impact of tab location on large format lithium-ion pouch cell based on fully coupled tree-dimensional electrochemical-thermal modeling, *Electrochimica Acta*, 147, 319–329.
- Schmidt O., Hawkes A., Gambhir A., Staffell I., 2017, The future cost of electrical energy storage based on experience rates, *Nature Energy*, 2, 1–8.
- Xu M., Zhang Z., Wang X., Jia L., Yang L., 2015, A pseudo three-dimensional electrochemical-thermal model of a prismatic LiFePO₄ battery during discharge process, *Energy*, 80, 303–317.
- Zhou S., Liu X., Hua Y., Zhou X., Yang S., 2021, Adaptive model parameter identification for lithium-ion batteries based on improved coupling hybrid adaptive particle swarm optimization- simulated annealing method, *Journal of Power Sources*, 482, 228951.